Korean J. Chem. Eng., **23**(5), 860-865 (2006)

Synthesis of ZnO nanowires on steel alloy substrate by thermal evaporation: Growth mechanism and structural and optical properties

Ahmad Umar, Jong-Pil Jeong*, Euk-Kyung Suh* and Yoon-Bong Hahn*,†

School of Chemical Engineering and Technology, and Nanomaterials Processing Research Centre,
*Department of Semiconductor Science and Technology, Chonbuk National University, Jeonju 561-756, Korea
(*Received 6 December 2005 • accepted 27 April 2006*)

Abstract−ZnO nanowires having a diameter in the range of 15-40 nm and several tens of micrometers in length were grown on steel alloy substrates by the thermal evaporation technique without the use of any catalyst or additives. A detailed structural analysis revealed that the as-grown ZnO nanowires are single crystalline with wurtzite hexagonal structures and preferentially oriented in the *c*-axis direction. Origination of a strong and sharp Raman-active E_2 mode at 436.6 cm^{-1} indicated that the grown ZnO nanowires have good crystal quality with the hexagonal wurtzite phase. Photoluminescence spectra also exhibited a sharp and strong peak in UV and a suppressed and weak band in the visible region, confirming the good optical properties and less structural defects for the deposited products. Additionally, a systematic growth mechanism is also proposed in detail to acquire a better understanding for the growth of nanowires on steel alloy substrate.

Key words: ZnO Nanowires, Thermal Evaporation, Steel Alloy Substrate

INTRODUCTION

Among II-VI semiconducting materials, a widely utilized ZnO has attracted much attention because of its captivating and dynamic properties. With a direct and wide band gap energy (3.37 eV) at room temperature, high breakdown strength and large exciton binding energy (60 meV), much larger than other semiconducting materials like ZnSe (22 meV) and GaN (25 meV), ZnO possesses several advantages for use in electronic and photonic devices [Kind et al., 2002; Huang et al., 2001; Lee et al., 2005]. The hexagonal wurtzite-structured ZnO has been investigated as a short wave-length light emitting, transparent conducting materials. Furthermore, a high piezoelectric constant of ZnO provides an opportunity for the fabrication of mechanical devices, for instance, acoustic transducers, sensors, and actuators [Verghese et al., 2000; Wang, 2003]. Different types of ZnO nanostructures have been reported in the literature to date [Sekar et al., 2005; Umar et al., 2005; Kim et al., 2004, 2005] which were synthesized by a number of fabrication techniques such as metal organic chemical vapor deposition (MOCVD) [Haga et al., 1999; Ogata et al., 2001], spray pyrolysis [Studenikin et al., 1998], ion beam assisted deposition [Li et al., 2000], laser ablation [Sum et al., 2004], sputter deposition [Chiou et al., 2003], template-assisted growth [Li et al., 2000], chemical vapor deposition (CVD) [Li et al., 2003] etc. A variety of substrates such as different orientations of silicon [Sekar et al., 2005; Umar et al., 2005; Kim et al., 2005], alumina [Wang, 2003], anodized aluminum oxide [Fang et al., 2003], CaF_2 [Liu et al., 2003], Au-coated stainless steel grid [Xu et al., 2005], indium doped tin oxide substrates, etc. have been used to grow the ZnO nanostructures. However, to the best of our knowledge, the synthesis of ZnO nanowires on steel alloy substrate is reported for the first time in this paper. Because of its resistance to acid corrosion, hardness when compared with other substrates and higher melting point, steel alloy is a promising substrate candidate for device fabrication. Additionally, the uniqueness in its surface morphology provides an excellent interaction between the substrate and the deposited nanostructures. As a new substrate, steel alloy offers a chance to study and determine the growth mechanism of the grown structures, which is quite interesting due to their special surface morphology. Among various kinds of ZnO nanostructures [Sekar et al., 2005; Umar et al., 2005; Kim et al., 2005; Haga et al., 1999; Ogata et al., 2001; Studenikin et al., 1998; Li et al., 2000, 2003; Sun et al., 2004; Chiou et al., 2003; Fang et al., 2003], the growths of one-dimensional ZnO nanowires hold a promising key for the fabrication of future optoelectronic and novel sensing devices. The interesting properties and versatile applications of ZnO have intrigued our group to work on this material.

In this paper, we report the synthesis of ZnO nanowires on steel alloy substrates at the temperature range of 550-650 °C by simple thermal evaporation method of high purity metallic zinc powder in the presence of oxygen. The as-grown ZnO nanowires on steel alloy substrate were characterized in terms of their structural and optical properties.

EXPERIMENTAL DETAILS

The commercially available steel alloy substrate (Fe: 72.8%, Cr: 22%, Al: 5%, Y: 0.1% and Zr: 0.1%) obtained from the "Good Fellow" London, U.K has been used for the growth of ZnO nanowires. A 1.5×1.5 cm sized steel alloy substrate was employed to grow ZnO nanowires using a thermal evaporation system, which consists of 50 cm long horizontal quartz tube with a halogen lamp heating system. The system was heated at the heating rate of 10 °C/s. A high purity metallic Zn powder (99.99%) and oxygen gas (99.999%) were used as a precursor of Zn and oxygen, respectively. The substrates were ultrasonically cleaned with alcohol and acetone sequen-

---

†To whom correspondence should be addressed.
E-mail: ybhahn@chonbuk.ac.kr

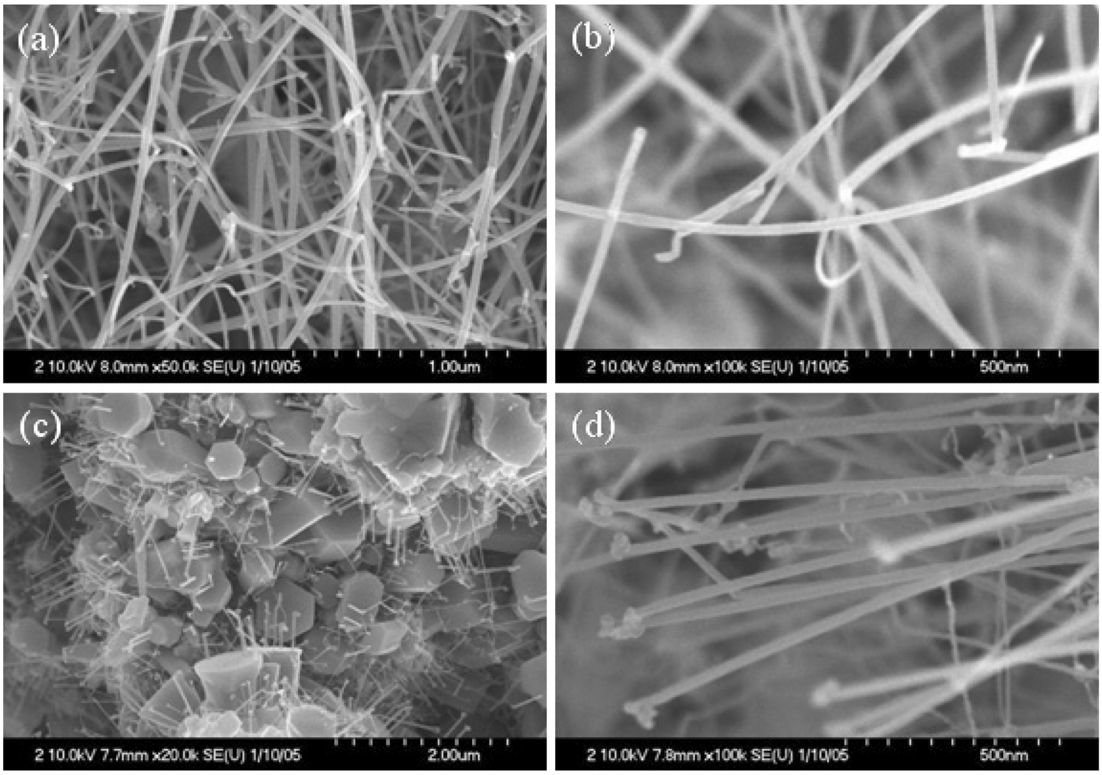

Fig. 1. (a) Low and (b) high magnified FESEM images of ZnO nanowires grown at the middle of the steel alloy substrate; (c) low and (d) high magnified images of the ZnO nanowires grown at the edge of the substrate.

tially. A thin layer of high purity metallic zinc powder was sprayed on this cleaned substrate and annealed on hot plate for 10 minutes prior to loading on the reaction chamber. After the sample was loaded, the chamber was evacuated to 1-4 Torr by using a rotary vacuum pump, which was slightly increased when the reactant gases were introduced into the reaction chamber. The substrates were pretreated by H_2 and N_2 gas for a period of 10-20 minutes with a 1 : 1 flow rate of each. After the pretreatment, high purity O_2 and N_2 gases were introduced inside the reactor with flow rates in the ratio of 2 : 1, respectively. The temperature for this synthesis ranges from 500-650 °C. The reaction lasted for about 100 minutes and a white colored product was deposited on the steel alloy substrates. To examine the annealing effect on the optical properties of the ZnO nanowires, the as-grown samples were annealed in an oxygen atmosphere in the same system at 450 °C for a period of 15 min.

The surface morphology of the deposited materials was investigated by field emission electron microscopy (FESEM) equipped with energy dispersive x-ray (EDX) spectrometry. The detailed structural characterization was done by using a transmission electron microscope (TEM, JEOL-JEM 2010, Curf) with the selected area electron diffraction (SAED) pattern. The crystallinity and phases of the grown nanowires were examined by the X-ray diffraction (XRD) pattern measured with Cu-Kα radiation. Room temperature Raman scattering and photoluminescence (PL) spectroscopy with the Ar^+ (513.4 nm), and He-Cd (325 nm) laser line as the exciton sources, respectively, were used to know the optical properties of the synthesized ZnO nanowires in detail.

RESULTS AND DISCUSSION

1. Detailed Structural Characterization of ZnO Nanowires Grown on Steel Alloy Substrate

The general morphology of the deposited materials was observed by using the FESEM images. Figs. 1 (a) and (b) show the low and high magnification images of as-grown product, which indicate that the ZnO nanowires have grown onto the steel alloy substrate in a high density. It can be seen from the images that most of the nanowires are in the diameter of 15-40 nm while their lengths are from several to tens of micrometers. These high aspect-ratio ZnO nanowires were observed from the middle portion of the substrate surface. In addition, some thinner and shorter with low aspect-ratio ZnO nanowires originated from the ZnO crystals have also been observed from both edge portions of the substrate. These shorter length nanowires are grown onto the hexagonal-shaped ZnO nanocrystals (Fig. 1(c)). The diameters of these hexagonal-shaped ZnO nanocrystals are 500-800 nm. Fig. 1(d) gives a sight for high magnification ZnO nanowires originating from the ZnO nanocrystals grown at the edge portions. The originating nanowires are perpendicular to the nanocrystals. The average diameters of these nanowires are 20-40 nm with the length of 1-2 μm. It is worthwhile to note that the appearances of different shaped ZnO nanowires at different positions of the substrates may be attributed to the difference in the growth temperature at different places of the substrate. It is very interesting to note that the observed nanowires show a metal nanoparticles on their tips; however, no metal catalyst or metallic additives were used to grow these ZnO nanowires. The presence of metal catalyst on the tips of the deposited structures indicates that the substrate surface itself provides some metal catalyst to facilitate the growth of the nanowires. The steel alloy substrate has several metals such

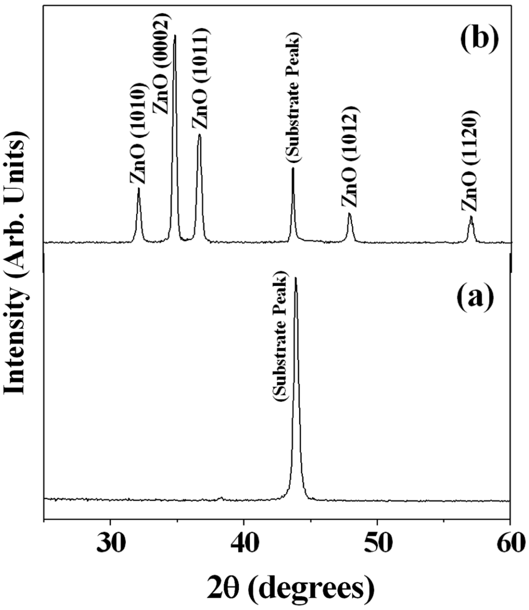

Fig. 2. XRD patterns of (a) steel alloy substrate and (b) ZnO nanowires grown on steel alloy substrate.

as Fe, Cr, Al, Y and Zr in a particular stoichiometric amount (shown in experimental section), so it is still unclear which metal particles are provided by the steel alloy substrate for the growing of the ZnO nanowires. Clearly, further study is required to obtain more conclusive evidence.

The crystallinity and crystal phase of the deposited materials were examined by the XRD patterns. Fig. 2(a) and (b) show the XRD patterns of the ZnO nanowires grown on the steel alloy and the bare steel alloy substrate, respectively. The indexed peaks in the spectrum correspond to the wurtzite hexagonal structure of the deposited materials and indicate that these are preferentially oriented in the c-axis direction. Furthermore, inception of one peak at 43.7° in the spectrum is due to the steel alloy substrate, which is confirmed by the XRD pattern in (b).

Detailed morphological and structural characterization of the grown ZnO nanowires on the steel alloy substrate was performed by using TEM combined with the SAED pattern. Figs. 3(a) and (b) show the low magnification TEM images, indicating the detailed morphology of the ZnO nanowires. It indicates that the nanowires are uniform in diameter throughout their length with a diameter of 20-30 nm. One interesting thing in these structures is that they show the metal nanoparticles capped on the tips of these nanowires, indicated by arrows, in spite of no use of metal catalyst during the growth process. Fig. 3(c) shows the high resolution TEM (HRTEM) image, presenting a detailed structural characterization of the grown ZnO nanowires. This image indicates that the grown structure is single crystalline with a lattice spacing of 0.52 nm which corresponds to the *d*-spacing of [0001] crystal planes of wurtzite ZnO. It confirms that the grown nanostructures are preferentially oriented in the *c*-axis direction. The SAED pattern projected along the [2110] zone axis (inset Fig. 3(c)) is consistent with the HRTEM image and indicates that the formed ZnO nanowires are grown along the [0001] direction.

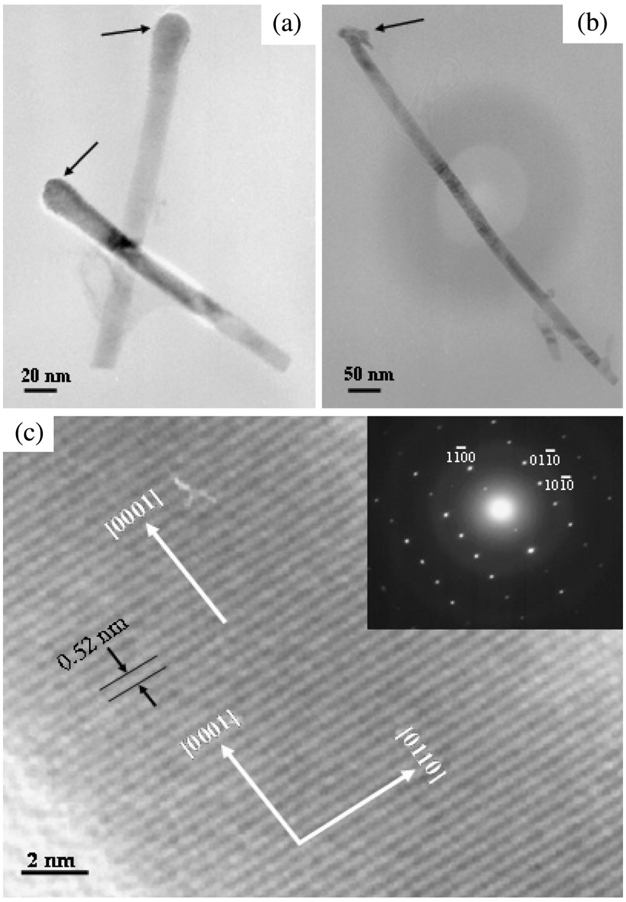

Fig. 3. Low magnification (a and b) and high-resolution (c) TEM images of ZnO nanowires grown on steel alloy substrate. The metal particles on the tips of the nanowires are indicated by the black arrows. Inset shows the corresponding SAED pattern.

2. Detailed Possible Growth Mechanism of ZnO Nanowires Grown on Steel Alloy Substrate

On the basis of the FESEM and TEM images (Fig. 1 and 3), a possible growth mechanism of the deposited ZnO nanowires on steel alloy substrate has been proposed. The growth of the nanowires follows two step processes: nucleation and growth. In the first step, during the hydrogen pretreatment, the nucleation occurs while the growth started in the second step when oxygen is introduced into the reactor chamber. Fig. 4 shows a detailed schematic possible growth mechanism for the formation of ZnO nanowires. First, a cleaned steel alloy substrate was coated with a thin layer of high purity metallic zinc powder, loaded into the reactor chamber and pretreated at 450 °C for 10-20 minutes in N_2 and H_2 environment. During this pretreatment step, the metallic zinc powder initially sprayed on the substrate started to melt (melting point 419.5 °C) and reacted with the steel alloy which led to the formation of zinc-metal alloy droplets (b). As the temperature increased up to 650 °C with the introduction of oxygen gas, this provided a sufficient environment for the growth of ZnO nuclei with the metal tips (c). Continuous introduction of oxygen gas and Zn source (obtained from the zinc powder sprayed on the substrate) leads to the formation of ZnO nanowires with the metal tips in a [0001] direction (d). Furthermore, it is also believed that the Zn or Zn sub-oxides play an important

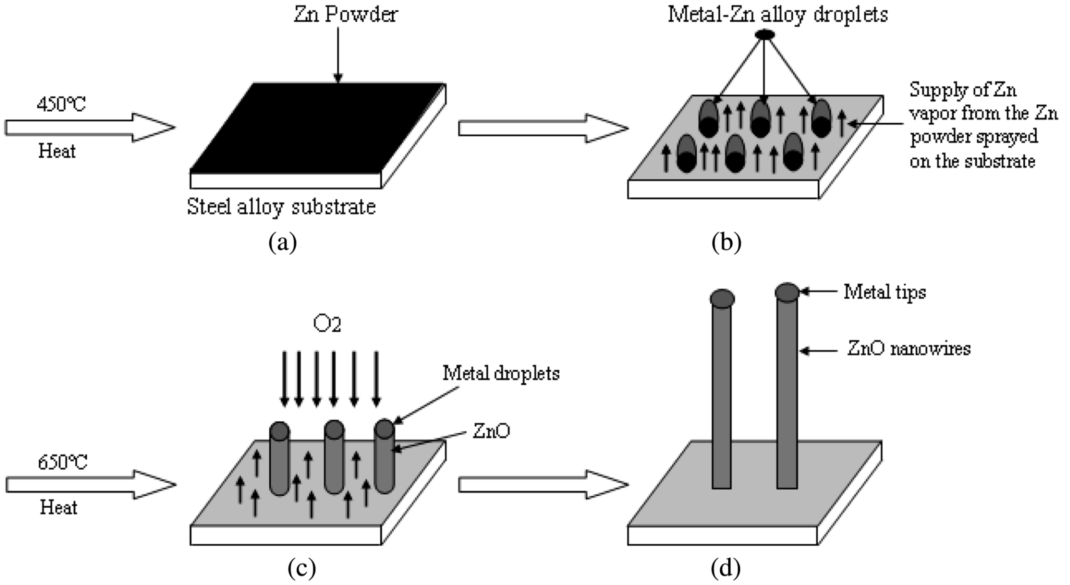

Fig. 4. Growth mechanism of the grown ZnO nanowires on steel alloy substrate: (a) metallic zinc powder coated on steel alloy substrate, (b) Zn particles on the substrate react with the steel alloy and form the zinc-metal droplets, (c) supply of O_2 and zinc from the substrate forms the ZnO nuclei with metal tips, (d) continuous feeding of O_2 and zinc vapor leads the formation of ZnO nanowires with metal tips.

role for the nucleation and growth of ZnO nanowires [Yao et al., 2002]. It is known that initially the Zn suboxides droplets form and these droplets can enhance the absorption and diffusion of zinc oxides [Wang et al., 2005]. So the diameter of the nanowires is determined by the size of the ZnO$_x$ drops. The wurtzite ZnO crystal is a polar crystal, and structurally the O^{2-} is arranged in hexagonal closest packing while the Zn^{2+} ions lie within a tetrahedral group of four oxygen ions. So the zinc and oxygen ions are arranged in a fourfold tetrahedral coordinated manner and stacked along the c-axis, alternatively. ZnO has positively charged Zn-(0001) terminated and negatively charged O-(0001) polar surfaces, in which the Zn-(0001) surface is chemically active for the growth of nanostructures while O-(0001) is inert. So the growth along the [0001] direction is dominated growth facet compared to others' growth facets such as {1011} and {1010} [Wang et al., 2003; Wang, 2004]. The obtained ZnO nanowires also exhibited growth in the [0001] direction, as was confirmed by the HRTEM, XRD and SEAD patterns. Interestingly, it was found that the nanowires exhibited metal nanoparticles at their tips even when no metal catalyst or metallic additives were used during the synthesis process. Hence, it is assumed that the appearance of these metal particles on the tip of nanowires was due to the steel alloy substrate which itself provides some metal catalyst to facilitate the growth of the nanowires.

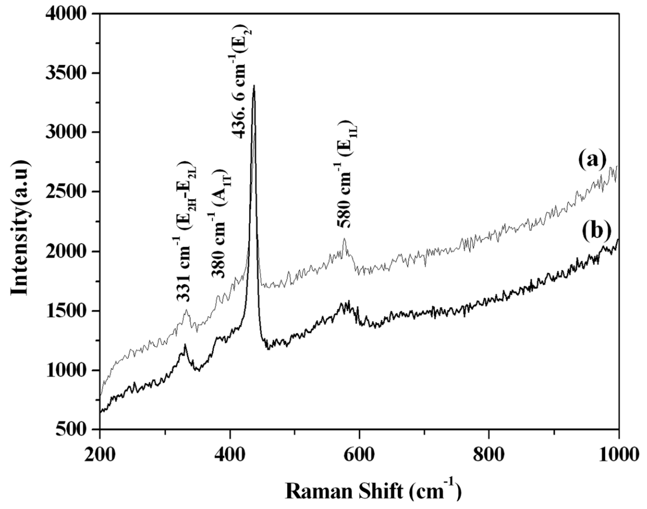

Fig. 5. Raman spectra for the ZnO nanowires grown on steel alloy substrates: (a) as-grown and (b) after annealing at 450 °C in an oxygen atmosphere for 15 min.

3. Detailed Optical Properties of ZnO Nanowires Grown on Steel Alloy Substrate

The optical properties of as-grown ZnO nanowires were done by the Raman-scattering and photoluminescence spectra at room temperature. The Raman spectra are sensitive to the crystallinity and the structural defects of the deposited nano and microstructures. ZnO having a wurtzite crystal structure belongs to the C_{6v}^4 with two formula unit primitive cells where all the atoms are occupying the C_{3V} sites. Among the eight sets of optical modes for single-crystalline ZnO, the A_1, E_1, and E_2 modes are Raman active. The E_2 modes are Raman active only while the A_1 and E_1 are infrared active and therefore split into two: longitudinal (LO) and transverse (TO) optical components [Calleja et al., 1977]. Fig. 5 shows the Raman scattering for the as-grown ZnO nanowires (a) and annealed (b) samples. A sharp and dominant peak was observed at 436.6 cm^{-1} attributed to be as Raman-active E_2 mode and characteristic of hexagonal wurtzite phase of ZnO [Ye et al., 2004]. The appearance of very short and suppressed peak at 580 cm^{-1} assigned to be as E_{1L}, originated due to the impurities and formation of defects such as oxygen vacancies, zinc interstitial and free carriers etc. In addition to these, two weak peaks at 331 cm^{-1} and 380 cm^{-1} were also observed and referred to as $E_{2H}-E_{2L}$ (multi phonon) and A_{1T} modes, respec-

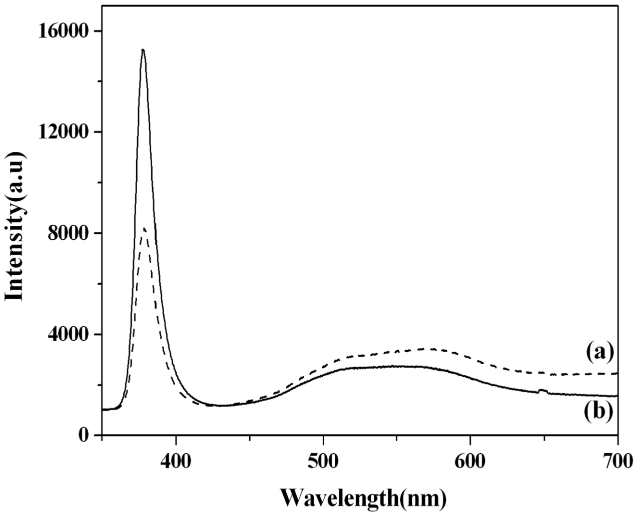

Fig. 6. Room temperature photoluminescence spectra for the ZnO nanowires: (a) as-grown (dotted line) and (b) after annealing (solid line) at 450 °C in an oxygen atmosphere for 15 min.

tively [Rajalakshmi et al., 2000]. The higher intensity and narrower spectral width of the Raman active E_2 mode compared with those of other observed peaks, confirming that the grown ZnO nanowires possess the wurtzite hexagonal phase with good crystal quality. To elucidate the annealing effect of the grown nanowires the samples were annealed in oxygen atmosphere at 450 °C for a period of 15 min. A higher intensity of Raman active E_2 mode was observed, at the same position (i.e., 436.6 cm^{-1}) from the annealed sample as compared to the as-grown. To explain this phenomenon Ye et al. reported that the annealing of ZnO in oxygen-rich environment enhances the intensity of Raman active E_2 mode due to the dominant effect of oxygen chemisorptions during the annealing process [Ye et al., 2004].

Fig. 6 shows the room temperature photoluminescence spectra of the (a) as-grown and (b) annealed ZnO nanowires on steel alloy substrate. Generally, two bands have been appearing in the PL spectra: in the UV region, called as near band edge (NBE) emission, originating due to the recombination of free-excitons through an exciton-exciton collision process and in the visible region recognized as deep level emission (DPE) caused by the impurities and structural defects in the crystal, for instance, oxygen vacancies and zinc interstitials etc. For the improvement of PL intensity of the as-grown products, the samples were annealed in an oxygen atmosphere at 450 °C for a period of 15 minutes. Both the samples exhibited two bands in the PL spectra: a sharp and strong UV emission at 379 nm and a suppressed and broad peak in the visible region, called as green emission, at 515-570 nm. In both the samples UV emission dominated over the green emission peaks. It is believed that the surface morphology and state of the synthesized nanostructures are sensitive and play an important role for the determination of PL spectra [Vanheusden et al., 1995]. The mechanism for the origination of green emission states that the green emission ascribed to the radial recombination of a photo-generated hole with electron of the singly ionized oxygen vacancies in the surface lattices of the ZnO [Vanheusden et al., 1996]. It is also reported that the radiative transitions between shallow donors (related to oxygen vacancies) and deep acceptors (zinc vacancies) can create defects in the luminescence spectra [Egehaff et al., 1996]. Additionally, the oxygen vacancies occur in three different charge states: the neutral oxygen vacancy, singly ionized oxygen vacancy and doubly ionized oxygen vacancies. Among these three oxygen vacancies, only the singly ionized oxygen vacancies can act as the luminescence centre [Kang et al., 2004]. It is observed that the reduction in oxygen vacancies can be achieved by annealing the samples in an oxygen-rich environment [Lim et al., 2004]. For annealing the synthesized ZnO nanowires we used a low temperature, i.e., 450 °C and it is known that at low annealing temperature the kinetic energy of atoms in the ZnO lattice is relatively low and the adsorption rate of the oxygen atoms is faster than the escaping rate. The oxygen enters into the ZnO crystal lattice sites, which improves the stoichiometric proportion of the synthesized product resulting in an enhancement in the crystal quality [Meng et al., 2005]. After annealing the samples in an oxygen atmosphere, we observed an enhanced PL intensity in the UV region with a suppressed peak in the visible region as compared to the pristine samples, which indicates that the level of the oxygen-related defects is reduced. The enhancement in the UV emission indicated an improvement in the crystal quality of the deposited ZnO nanowires. Bagnall et al. have reported that the crystallinity is an important factor to enhance a strong near band edge emission [Bagnall et al., 1998]. So the decrease in impurities and structural defects such as oxygen vacancies and zinc interstitials leads to the enhancement in UV emission intensity with a decrease in the deep level intensity. The appearance of sharp and strong near band edge emission in the UV region and a suppressed but broad deep level emission in the visible region indicated that the as-grown ZnO nanowires showed a good crystallinity with a good optical property with few structural defects such as oxygen vacancies and interstitials of zinc.

CONCLUSION

ZnO nanowires of a high density and good crystallinity have been synthesized on steel alloy substrate, for the first time, by the simple thermal evaporation method using metallic zinc powder and oxygen gas as a source material for zinc and oxygen, respectively. The obtained ZnO nanowires are 15-40 nm in diameter and several to tens of micrometers in length. Detailed structural investigation indicated that the grown nanowires are single crystalline having the hexagonal wurtzite structure and are preferentially oriented in the c-axis in [0001] direction. The detailed growth mechanism indicates that the steel alloy substrate itself is responsible for the appearance of metal tips on the end of the nanowires. Raman spectra confirm that the grown ZnO nanowires have good crystal quality with the wurtzite hexagonal phase. Room temperature PL spectra also show a sharp and strong peak in the UV region and a suppressed and weak band in the visible region, indicating that the as-grown products have good optical properties with less structural defects. Annealing the as-grown ZnO nanowires in oxygen atmosphere enhances the crystal quality and optical properties of the ZnO nanowires.

ACKNOWLEDGMENTS

This work was supported by the Basic Research Program of the Korea Science and Technology Foundation (R01-2006-000-4306-

0). A. Umar is grateful to the Korea Research Foundation (KRF) for its graduate research fellowship program.

REFERENCES

Bagnall, D. M., Chen, Y. F., Zhu, Z., Yao, T., Shen, M. Y. and Goto T., "High temperature excitonic stimulated emission from ZnO epitaxial layers," *Appl. Phys. Lett.*, **73**, 1038 (1998).

Calleja, J. M. and Cardona, M., "Resonant Raman scattering in ZnO," *Phys. Rev. B*, **16**, 3753 (1977).

Chiou, W., Wu, W. and Ting, J., "Growth of single crystal ZnO nanowires using sputter deposition," *Diamond Relat. Mater.*, **12**, 1841 (2003).

Egehaaf, H. J. and Oelkrug, D., "Luminescence and nonradiative deactivation of excited states involving oxygen defect centers in polycrystalline ZnO," *J. Crystal Growth*, **161**, 190 (1996).

Fang, Z., Wang, Y., Peng, X., Liu, X. and Zhen, C., "Structural and optical properties of ZnO films grown on the AAO templates," *Materials Letters*, **57**, 4187 (2003).

Haga, K., Katahira, F. and Watanabe, H., "Preparation of ZnO films by atmospheric pressure chemical-vapor deposition using zinc acetylacetonate and ozone," *Thin Solid Films*, **343-344**, 145 (1999).

Huang, M., Mao, S., Feick, H., Yan, H., Wu, Y., Kind, H., Weber, E., Russo, R. and Yang, P., "Room-temperature ultraviolet nanowire nanolasers," *Science*, **292**, 1897 (2001).

Kang, H. S., Kang, J. S., Kim, J. W. and Lee, S. Y., "Annealing effect on the property of ultraviolet and green emissions of ZnO thin films," *J. Appl. Phys.*, **95**, 1246 (2004).

Kim, S. H., Umar, A. and Hahn, Y. B., "Growth and formation mechanism of sea-urchin like ZnO nanostructures on Si," *Korean J. Chem. Eng.*, **22**, 489 (2005).

Kim, T. Y., Lee, S. H., Mo, Y. H., Nahm, K. S., Kim, J. Y., Suh, E. K. and Kim, M., "Growth mechanism of needle-shaped ZnO nanostructures over NiO-coated Si substrates," *Korean J. Chem. Eng.*, **21**, 733 (2004).

Kind, H., Yan, H., Messer, B., Law, M. and Yang, P., "Nanowire ultraviolet photodetectors and optical switches," *Adv. Mater.*, **14**, 158 (2002).

Lee, S., Im, Y. H. and Hahn, Y. B., "Two-step growth of ZnO films on silicon by atomic layer deposition," *Korean J. Chem. Eng.*, **22**, 334 (2005).

Li, S. Y., Lee, C. Y. and Tseng, T. Y., "Copper-catalyzed ZnO nanowires on silicon (100) grown by vapor-liquid-solid process," *J. Cryst. Growth*, **247**, 357 (2003).

Li, W., Mao, D. S., Zheng, Z. H., Wang, X., Liu, X. H., Zou, S. C., Zhu, Y. K., Li, Q. and Xu, J. F., "ZnO/Zn phosphor thin films prepared by IBED," *Surf. Coat. Technol.*, **128/129**, 346 (2000).

Li, Y., Meng, G. W. and Zhang, L. D., "Ordered semiconductor ZnO nanowire arrays and their photoluminescence properties," *Appl. Phys. Lett.*, **76**, 2011 (2000).

Lim, J., Shin, K., Kim, H. W. and Lee, C., "Effect of annealing on the photoluminescence characteristics of ZnO thin films grown on the sapphire substrate by atomic layer epitaxy," *Mater. Sci. Eng. B*, **107**, 301 (2004).

Liu, Y. C., Xu, X. Y., Mu, R., Henderson, D. O., Lu, Y. M., Zhang, J. Y., Shen, D. Z., Fan, X. W. and White, C. W., "Production, structure, and optical properties of ZnO nanocrystals embedded in CaF_2 matrix," *Appl. Phys. Lett.*, **83**, 1210 (2003).

Meng, X. Q., Shen, D. Z., Zhang, J. Y., Zhao, D. X., Lu, Y. M., Dong, L., Zhang, Z. Z., Liu, Y. C. and Fan, X. W., "The structural and optical properties of ZnO nanorod arrays," *Solid State Communications*, **135**, 179 (2005).

Ogata, K., Kawanishi, T., Maejima, K., Sakurai, K., Fujita, S. and Fujita, S., "Improvements of ZnO qualities grown by metal-organic vapor phase epitaxy using a molecular beam epitaxy grown ZnO layer as a substrate," *Jpn. J. Appl. Phys. Part-2*, **40**, L657 (2001).

Rajalakshmi, M., Arora, A. K., Bendre, B. S. and Mahamuni, S., "Optical phonon confinement in zinc oxide nanoparticles," *J. Appl. Phys.*, **87**, 2445 (2000).

Sekar, A., Kim, S. H., Umar, A. and Hahn, Y. B., "Catalyst-free synthesis of ZnO nanowires on Si by oxidation of Zn powders," *J. Crystal Growth*, **277**, 471 (2005).

Studenikin, S. A., Golego, N. and Cocivera, M., "Fabrication of green and orange photoluminescence undoped ZnO films using spray pyrolysis," *J. Appl. Phys.*, **84**, 2287 (1998).

Sun, Y., Fuge, G. M. and Ashfold, M. N. R., "Growth of aligned ZnO nanorod arrays by catalyst-free pulsed laser deposition methods," *Chem. Phys. Lett.*, **396**, 21 (2004).

Umar, A., Kim, S. H., Lee, Y.-S., Nahm, K. S. and Hahn, Y. B., "Catalyst free large-scale synthesis of ZnO nanorods by a vapor-solid growth mechanism: Structural and optical properties," *J. Crystal Growth*, **282**, 131 (2005).

Umar, A., Lee, S., Im, Y. H. and Hahn, Y. B., "Flower-shaped ZnO nanostructures obtained by cyclic feeding chemical vapor deposition: Structural and optical properties," *Nanotechnology*, **16**, 2462 (2005).

Umar, A., Lee, S., Lee, Y. S., Nahm, K. S. and Hahn, Y. B., "Star-shaped ZnO nanostructures on silicon by cyclic feeding chemical vapor deposition," *J. Crystal Growth*, **277**, 479 (2005).

Vanheusdan, K., Seager, C. H., Warren, W. L., Tallent, D. R. and Voigt, J. A., "Correlation between photoluminescence and oxygen vacancies in ZnO phosphors," *Appl. Phys. Lett.*, **68**, 403 (1995).

Vanheusdan, K., Warren, W. L., Seager, C. H., Tallent, D. R., Voigt, J. A. and Gnade, B. E., "Mechanism behind green photoluminescence in ZnO phosphor powders," *J. Appl. Phys.*, **79**, 7983 (1996).

Verghese, P. M. and Clarke, D. R., "Piezoelectric contributions to the electrical behavior of ZnO varistors," *J. Appl. Phys.*, **87**, 4430 (2000).

Wang, F. Z., Ye, Z. Z., Ma, D. W., Zhu, L. P. and Zhuge F., "Novel morphologies of ZnO nanotetrapods," *Materials Letters*, **59**, 560 (2005).

Wang, Z. L., "Nanostructures of zinc oxide," *Materials Today*, **7**(6), 26 (2004).

Wang, Z. L. (Ed.), "Nanowires and Nanobelts - Materials, Properties and Devices, Metal and Semiconductor Nanowires," vol. I and vol. II Kluwer Academic Publisher, Dordrecht (2003).

Wang, Z. L., Kong, X. Y. and Zuo, J. M.,"Induced growth of asymmetric nanocantilever arrays on polar surfaces," *Phys. Rev. Lett.*, **91**, 185502 (2003).

Xu, X. Y., Zhang, H. Z., Zhao, Q., Chen, Y. F., Xu, J. and Yu, D. P., "Patterned growth of ZnO nanorod arrays on a large-area stainless steel grid," *J. Phys. Chem. B*, **109**, 1699 (2005).

Yao, B. D., Chan, Y. F. and Wang, N., "Formation of ZnO nanostructures by a simple way of thermal evaporation," *Appl. Phys. Lett.*, **81**, 757 (2002).

Ye, J. D., Gu, S. L., Zhu, S. M., Qin, F., Liu, S. M., Liu, W., Zhou, X., Hu, L. Q., Zhang, R., Shi, Y. and Zheng, Y. D., "Production of high-quality ZnO films by the two-step annealing method," *J. Appl. Phys.*, **96**, 5308 (2004).